ChemPubSoc Europe
DOI: 10.1002/cphc.201600993
Articles

Platinum Inhibits Low-Temperature Dry Lean Methane Combustion through Palladium Reduction in Pd–Pt/Al_2O_3: An In Situ X-ray Absorption Study

Hanieh Nassiri,[a] Kee-Eun Lee,[b, c] Yongfeng Hu,[c] Robert E. Hayes,[a] Robert W. J. Scott,[b] and Natalia Semagina*[a]

Palladium–platinum bimetallic catalysts supported on alumina with palladium/platinum molar ratios ranging from 0.25 to 4 are studied in dry lean methane combustion in the temperature range of 200 to 500 °C. Platinum addition decreases the catalyst activity, which cannot be explained by the decrease in dispersion or the structure sensitivity of the reaction. In situ X-ray absorption near-edge structure and extended X-ray absorption fine structure spectroscopy measurements have been conducted for monometallic Pd, Pt, and 2:1 Pd–Pt catalysts. Monometallic palladium is fully oxidized in the full temperature range, whereas platinum addition promotes palladium reduction, even in a reactive oxidizing environment. The Pd/PdO weight ratio in bimetallic Pd–Pt 2:1 catalysts decreases from 98/2 to 10/90 in the 200–500 °C temperature range under the reaction conditions. Thus, platinum promotes the formation of the reduced palladium phase with a significantly lower activity than that of oxidized palladium. The study sheds light on the effect of platinum on the state of the active palladium surface under low-temperature dry lean methane combustion conditions, which is important for methane-emission control devices.

1. Introduction

Catalyst development for low-temperature natural-gas (NG) combustion has received significant attention because of the forecasted increase in NG-fueled devices[1] and the need for efficient emission control of methane with a greenhouse gas potential exceeding that of CO_2 by 23 times.[2] There are many examples of methane emissions that encompass a wide range of conditions. For example, increasing interest in NG-fueled vehicles has increased demand for an effective catalyst that can oxidize methane in a lean wet environment. There are also numerous examples of fugitive CH_4 emission sources that are lean and dry. A large source of methane emissions is the vent gas from underground coal mines that is burned to produce heat.[3] The oil and gas industry also has many fugitive emission sources, including emissions from NG compressor stations and the vent gas from oil wells.[2] The volumetric efficiency and operating temperature range of current palladium-based catalysts require improvement for successful device commercialization, which promotes the search for suitable metal promoters and supports.[2,4]

[a] H. Nassiri, Prof. R. E. Hayes, Prof. N. Semagina
Department of Chemical and Materials Engineering
University of Alberta
9211-116 St., Edmonton, Alberta T6G 1H9 (Canada)
E-mail: semagina@ualberta.ca
[b] Dr. K.-E. Lee, Prof. R. W. J. Scott
Department of Chemistry
University of Saskatchewan
110 Science Place, Saskatoon, Saskatchewan, S7N 5C9 (Canada)
[c] Dr. K.-E. Lee, Dr. Y. Hu
Canadian Light Source Inc.
44 Innovation Boulevard, Saskatoon, Saskatchewan S7N 2V3 (Canada)

The active chemical state of palladium in lean methane combustion has been a matter of debate. The turnover rates increased by an order of magnitude with a threefold increase in the Pd/PdO_x ratio, as measured by NH_3 temperature-programmed desorption (TPD), and the coexistence of metallic Pd with PdO was claimed to be paramount.[5] However, a further ratio increase to five was found to be detrimental to catalytic activity.[5] Farrauto et al. showed a loss of activity when metallic palladium was formed under reducing reaction conditions.[6] The group of Iglesia reported that the methane oxidation rate coefficients at various oxygen pressures at 700 °C were a single function of total oxygen content in Pd/Al_2O_3 catalysts with nanoparticle sizes from 1.8 to 8.8 nm.[7] The conclusion was drawn from oxygen uptake and evolution measurements, methane combustion kinetic measurements, and thermodynamic calculations. Using in situ extended X-ray absorption fine structure (EXAFS) measurements, Grunwaldt et al. detected the presence of metallic Pd on a Pd/ZrO_2 catalyst at 500–550 °C and suggested its beneficial effect, considering that the activity of prereduced catalyst was higher than that of the oxidized catalyst.[8] An operando Raman study of the Pd/Al_2O_3 catalyst in the 25–500 °C range detected only palladium oxide forming under the reaction conditions;[9] this is consistent with thermodynamic expectations and the kinetic investigation of Pd/ZrO_2 catalysts by Fujimoto et al.[10] The latter study explained the frequently reported requirement of the coexistence of Pd–PdO_x by a Mars–van Krevelen mechanism when CH_4 is activated on site pairs consisting of O atoms and O vacancies on the PdO_x surface. These vacancies can also be easily poisoned by water, which is known for its strong inhibitory

effect on palladium-catalyzed methane combustion. Thus, knowledge of the required chemical state of palladium under the reaction conditions and the ability to control it, if necessary, is paramount to designing an efficient and stable NG combustion catalyst.

In the quest for a suitable promoter to enhance the performance of palladium in methane combustion, platinum has been extensively used.[11–15] Monometallic platinum is a poor methane combustion catalyst under lean conditions.[16] In an oxidative atmosphere, Pt on a γ-alumina support is more susceptible to sintering than Pd; thus, in Pd–Pt formulations, Pd stabilizes Pt as a result of strong interactions between PdO and the support.[17,18] In bimetallic catalysts, the chemical states of palladium and platinum can be affected by their ratios, preparation methods, and catalyst support to enhance or suppress methane conversion.[13,15,19–25] The reactivities of palladium and platinum towards oxygen depend on the temperature and partial pressure of oxygen,[7,17,26–29] metal support,[27,30] and nanoparticle size.[7,31] In addition to metallic Pd and Pt, oxide species, such as PdO, PdO_2, PtO, PtO_2, and Pt_3O_4, may be present.[32–35] In bimetallic catalysts, the formation of mixed-oxide phases of $Pd_xPt_{1-x}O_y$ was shown through DFT calculations by Dianat et al.[35] The addition of platinum to palladium was suggested to stabilize the higher oxidation state of palladium. The oxygen-binding energy in the Pd–Pt catalysts was found to be higher on palladium-rich surfaces because of charge transfer from Pd to Pt atoms.[36] The extent of palladium segregation to the surface after oxidative aging at 750 °C was found to be insignificant in one study,[37] but was claimed to be important in another.[38]

An improvement in the dissociation of methane and oxygen adsorption was suggested by Persson et al. to be the reason for the higher activity of bimetallic Pd–Pt catalysts as compared to monometallic Pd.[32] Kinnunen et al. believed that the proportions of metal and metal oxide surface sites determined the catalytic activity when a small amount of Pt was necessary to enhance the low-temperature conversion, but a higher Pt content was detrimental due to the suppressed reoxidation of Pd.[11] Thermogravimetric analysis of Pd, Pt, and Pd–Pt catalysts in air showed that Pt stabilized Pd in its reduced form and shifted the onset of deactivation by PdO→Pd transformation to lower temperatures in the range of 850–950 °C, leading to lower intrinsic activity in lean methane combustion.[14] At the same time, Pt improved the sintering resistance of Pd, which resulted in an overall beneficial effect on methane combustion at low Pt loadings (Pt mass fraction $<10\%$).[14] In line with these observations, an ex situ X-ray absorption (XAS) study of Pd–Pt catalysts oxidized at 750 °C revealed that Pt helped Pd to maintain its reduced form when only 20–30% of Pd was present in its oxide form.[37]

The reported observations of the effect of platinum on palladium covered temperatures above 600 °C,[14,37] which is beyond the range of interest for low-temperature methane combustion, and did not investigate the metal chemical states under the reaction conditions. Herein, we shed light on the effect of Pt on Pd/PdO_x distribution in $Pd–Pt/Al_2O_3$ methane combustion catalysts in a low-temperature range of interest (200–550 °C) through an in situ XAS study and the effect of reduced Pd on dry lean methane combustion.

2. Results and Discussion

Table 1 summarizes the range of synthesized Pd–Pt and monometallic catalysts supported on commercial γ-Al_2O_3 and their dispersions, as determined from CO chemisorption. The catalyst notation is based on the molar ratio of the two metals and reflects the metal loadings determined by NAA. The samples were precalcined in air at 550 °C for 16 h, which is a recommended commercial procedure preceding automotive catalytic converter testing for lean burn applications. For the dispersion determination, a 1:1 stoichiometry of the adsorbed CO per surface mole of Pd and/or Pt was assumed.

Table 1. Characteristics of the synthesized catalysts supported on γ-Al_2O_3.

Catalyst	Pd/Pt molar ratio	Loading[a] [wt%] Pd	Pt	Dispersion[b] [%]	CH_4 conversion at 350 °C[c] [%]
Pd	–	0.2550	–	43	52
Pd/Pt 4:1	4	0.1780	0.0772	53	65
Pd/Pt 2:1	2	0.1520	0.1240	31	28
Pd/Pt 1:1	1	0.0875	0.1700	23	15
Pd/Pt 1:2	0.5	0.0659	0.1910	20	14
Pd/Pt 1:4	0.25	0.0328	0.2150	16	4
Pt	0	–	0.295	13	1

[a] Determined by neutron activation analysis (NAA). [b] From CO chemisorption by assuming a 1:1 stoichiometry of CO/metal. [c] Pd amounts in all tests were kept at 1.2 mg; 1.2 mg of monometallic Pt was used. An intrinsic kinetic regime under isothermal operation at 350 °C was confirmed.

As expected,[39] the addition of palladium to platinum prevented its excessive sintering, which also can be seen in the TEM images of the calcined catalysts (Figure 1). A richer palladium content of the catalysts results in a lower degree of sintering.

The catalysts were tested in dry lean methane combustion, and the corresponding methane conversions in the temperature-programmed reactions are shown in Figure 2.

Only the first ignition curve is reported for each catalyst, the duration of which is short enough compared with precalcination for 16 h at 550 °C, so that the effect of in situ restructuring may be considered negligible. The curve for monometallic pre-

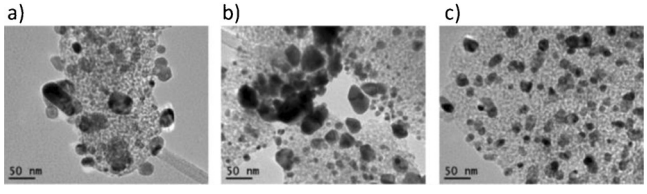

Figure 1. TEM images of the calcined supported catalysts: a) Pd, b) Pt, and c) Pd–Pt 2:1.

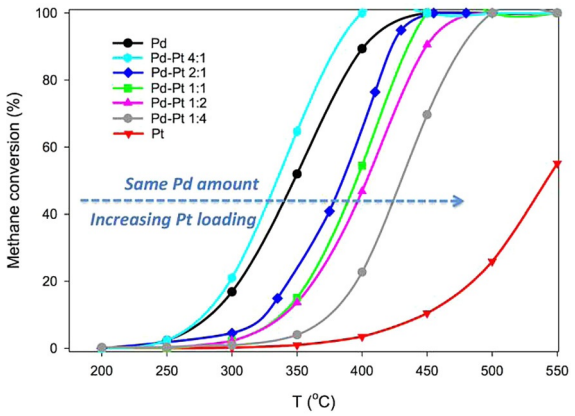

Figure 2. Ignition curves recorded in the dry lean methane combustion. Palladium amounts in all tests were kept at 1.2 mg, except for monometallic Pt (also 1.2 mg). The curve for monometallic prereduced palladium is not shown because it is identical to that of oxidized Pd, within 3% error.

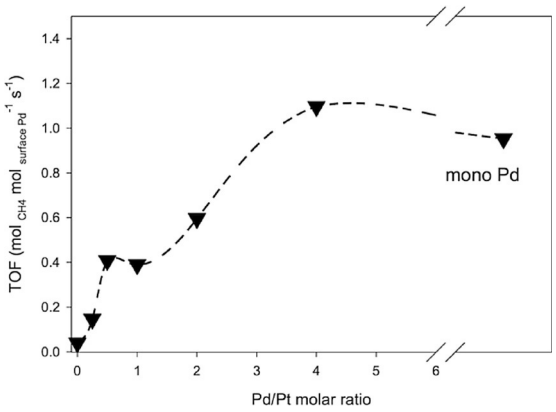

Figure 3. Initial TOFs normalized per surface Pd atom (or Pt for monometallic Pt) at 350 °C as a function of Pd/Pt ratio by assuming the same surface and bulk composition.

reduced palladium is not shown because it is identical to that of oxidized palladium within a 3% error. Monometallic platinum shows extremely low activity relative to that of palladium; platinum is indeed known for efficient methane combustion only under fuel-rich conditions.[16] Because Pt showed very low activity, all tests with monometallic Pd and bimetallic Pd–Pt catalysts were performed at the same Pd loading in the reactor (1.2 mg). The methane conversions at 350 °C are also summarized in Table 1.

Clearly (Table 1 and Figure 2), a higher Pd–Pt ratio results in more efficient combustion at lower temperatures. Because metal dispersions also increase with the ratio, a hypothesis on the negative effect of Pt due to larger particle size was verified by calculating the catalyst activity per mole of surface Pd atoms because of its significantly higher activity than that of Pt. Assuming for now the structure-insensitive reaction, surface-normalized activities [turnover frequency (TOF)] should stay constant per active component, irrespective of nanoparticle size. For the calculation, first order in methane and zero order in hydrogen were assumed,[10] and the rate constants found were used to calculate the initial reaction rates at 350 °C (Figure 3).

As seen in Figure 3, the surface-normalized activities drop by an order of magnitude with increasing platinum content in the bimetallic catalysts, which indicates that platinum does not simply dilute the active palladium surface. Palladium-surface-normalized activities were calculated based on the assumption of the same surface Pd–Pt ratio as that in the bulk. The extent of palladium segregation to the surface after oxidative aging at 750 °C was found to be insignificant in one study,[37] but was claimed to be important in another.[38] If it occurred, the decrease in palladium-surface-normalized activity with platinum addition would be even more dramatic.

Palladium-catalyzed methane combustion is known as a structure-sensitive reaction, with a 65-fold increase in TOF with palladium dispersion decrease from 50 to 10%.[27] Herein, the TOF for the monometallic Pd catalyst has the largest value, although the dispersion in some Pd–Pt catalysts decreases to 16% upon Pt addition (Table 1). Thus, the effect of platinum addition cannot be explained by the structure sensitivity of the reaction either, which should bring about an increase rather than a decrease in TOF.

To shed light on the mechanism of the effect of Pt, in situ X-ray absorption near-edge structure (XANES) and EXAFS spectroscopy measurements were conducted for the monometallic Pd and Pt catalysts and the Pd–Pt 2:1 catalyst, which represented the central point of the negative effect of Pt (Figures 2 and 3) with dispersion (31%); this is similar to that of Pd (43%). The measurements were performed in a dry lean methane/air mixture (O_2/CH_4 molar ratio of 134, <1 ppm H_2O) over a temperature range of 200 to 500 °C and compared with standard materials (Pd and Pt foils and PdO). Figure 4 shows the

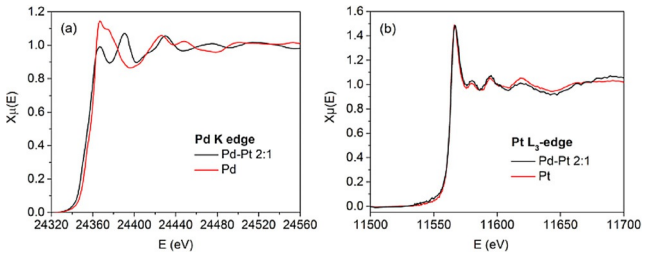

Figure 4. XANES spectra of calcined Pd and Pd–Pt 2:1 samples before the methane combustion reaction: a) Pd K edge and b) Pt L_3 edge.

Pd K- and Pt L_3-edge XANES spectra of the calcined Pd, Pt, and Pd–Pt samples before the reaction. The Pd K-edge XANES probes the electronic transition from the 1s to 5p orbitals and is sensitive to both oxidation state and coordination environment of the Pd atoms.[40] The calcined Pd–Pt 2:1 sample compared well to that of the Pd foil, which indicated that the majority of Pd was in the zero-valent state. On the contrary, the spectrum of the calcined monometallic Pd sample resembled that of PdO, which implied that Pd was mostly oxidized to Pd^{II} in this sample. Thus, the presence of Pt in bimetallic Pd–Pt particles leads to the stabilization of Pd^0 in the particles towards oxidation; this is in agreement with what is already

known for calcined Pd–Pt systems.[14,37] The Pt L_3-edge XANES spectra showed the same features between the Pt and Pd–Pt 2:1 samples, which indicated that there was no difference in the oxidation state of Pt upon Pd addition.

The in situ measurement under a CH_4/dry air mixture shows a substantial change in the speciation of Pd upon increases in temperature. The calcined Pd sample consisted only of PdO; thus, to compare it with the bimetallic catalyst containing mostly Pd^0, reduction of the monometallic Pd catalyst was conducted at 350 °C for 2 h under a stream of H_2 gas. Figure 5

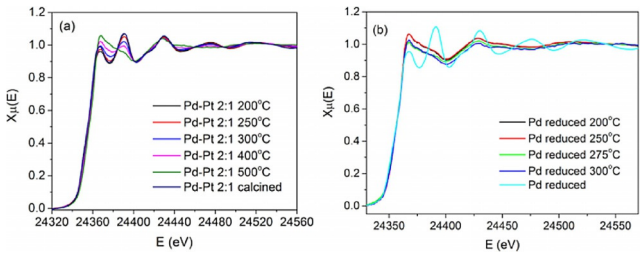

Figure 5. XANES spectra under CH_4/dry air conditions for a) calcined Pd–Pt 2:1 and b) reduced Pd.

shows the Pd K-edge in E space for the supported Pd and Pd–Pt 2:1 under in situ CH_4/dry air conditions. The spectra were collected at incrementally increasing temperatures in methane/air flows. Upon increasing the temperature, the Pd–Pt 2:1 sample slowly became more oxidized, whereas rapid oxidation was seen in the monometallic Pd sample. To understand the change in speciation of Pd in the Pd–Pt 2:1 and Pd samples, linear combination fitting with Pd^0 and PdO standards was performed at each temperature; the results are shown in Table 2 and Figure 6.

Linear combination fitting shows that the Pd–Pt 2:1 sample was slightly oxidized at 200 °C under CH_4/dry air conditions, and the level of oxidation increased linearly up to 90% at 500 °C. Even at 500 °C, significant amounts of Pd^0 are still present in these particles. The Pd–Pt 2:1 sample still showed the metallic Pd feature with a slightly decreased intensity and an edge shift, which was not observed in the Pd/Al_2O_3 sample. The EXAFS results below also verify that small amounts of Pd^0 are still present in the bimetallic sample. In the case of the reduced monometallic Pd sample, nearly complete Pd oxidation to PdO is seen at 200 °C, which is complete by 250 °C, and there are no further spectral changes beyond that temperature. It is known that surface palladium oxidation is complete at room temperature and bulk oxidation is diffusion limited and takes place at 200–700 °C.[41] The ignition curve measured for the prereduced palladium catalyst was identical to that of the oxidized catalyst (Figure 2; within a 3% conversion variation as a typical measurement error), in agreement with the in situ XAS results.

Table 2. Linear combination fitting for the Pd/Pt 2:1 sample in CH_4/dry air environment.

Reaction *T* [°C]	Pd^{II} from PdO [wt%]	Pd^0 [wt%]
before reaction, calcined	<2	>98
200	4	96
250	16	84
300	37	63
400	62	38
500	90	10

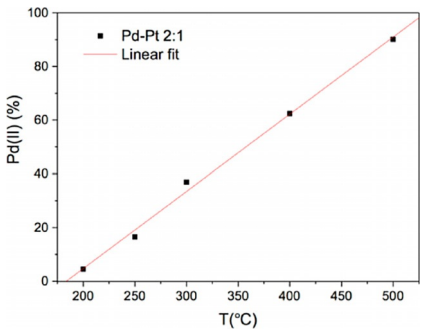

Figure 6. Linear combination fitting results of the Pd K-edge XANES spectra showing the percentage of PdO formed as a function of temperature in CH_4/dry air environment.

Figure 7 shows the Fourier-transformed Pd K-edge EXAFS plot in R space as a function of temperature for the Pd–Pt and reduced Pd samples under in situ CH_4/dry air conditions. The peaks in the 1.9 to 2.5 Å range correspond to first-shell Pd–Pd

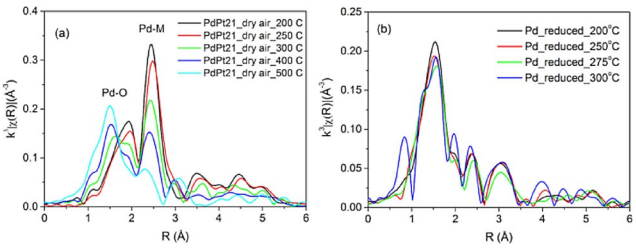

Figure 7. Pd K-edge EXAFS spectra in R space for a) Pd–Pt 2:1 and b) reduced Pd in CH_4/dry air environment.

and Pd–Pt contributions, whereas the peak at 1.5 Å corresponds to Pd–O first-shell contributions. For the Pd–Pt 2:1 sample, the amplitude of the Pd–Pd and Pd–Pt contributions decreases, while a new Pd–O contribution emerges beyond 300 °C, which agrees well with the above linear-combination fitting data. Platinum EXAFS data showed no changes over the entire temperature range examined (not shown). For the Pd K-edge data shown in Figure 7a, the intensity of the Pd–M peaks is reduced in amplitude and broadened at higher temperatures due to increased thermal disorder in the sample. As a consequence of this thermal broadening, it was not possible to fit EXAFS data accurately at various temperatures to extract quantitative coordination numbers for each of the Pd–O, Pd–Pd, and Pd–Pt contributions. The Pd–Pt 2:1 sample at 500 °C shows a significant Pd–O contribution, but still retains weak Pd–M contributions. In addition, a weak second-shell Pd–Pd contribution from PdO is seen at about 3 Å for the

500 °C bimetallic sample. Figure 7b shows the Pd K-edge EXAFS plot in the R space of the reduced monometallic Pd sample at various temperatures under CH_4/dry air conditions; beyond 200 °C, the EXAFS mainly shows the Pd–O first-shell contribution at 1.5 Å and a second-shell Pd–Pd contribution at 3.0 Å (due to PdO). This agrees with the above XANES data, which showed that the pure palladium sample was nearly completely oxidized by 200 °C.

Thus, the in situ XAS studies revealed that 1) irrespective of the initial reduced or oxidized state of Pd, only PdO existed at 200–500 °C under oxidative reaction conditions; 2) the state of Pt was not affected by the presence of Pd and did not change under the reaction conditions; and 3) the Pd/PdO weight ratio in bimetallic Pd–Pt 2:1 catalysts decreased from 98/2 to 10/90 in the 200–500 °C range during combustion.

By coupling these observations with the kinetic data indicating the negative effect of the addition of Pt to the performance of the Pd catalyst, which is not connected to surface dilution, size effects, or structure sensitivity (Figures 2 and 3 and Table 1), it follows that Pt promotes the formation of a reduced Pd phase, which is significantly less active than that in the methane combustion reaction, as opposed to the oxidized Pd. A similar negative effect of metallic palladium was reported by Farrauto et al.,[6] and the active oxidized palladium working state was also claimed in an operando Raman study.[9] Metallic Pd is characterized by a higher activation barrier for C–H bond activation in methane than that in PdO clusters.[42] The current study provides in situ evidence of the importance of oxidized palladium and its dependence on the presence of platinum for dry lean methane combustion in the 200–500 °C temperature range.

3. Conclusions

Pd–Pt/γ-Al_2O_3 catalysts with Pd/Pt molar ratios of 0.25 to 4 were studied in dry lean methane combustion in the temperature range of 200–500 °C, along with monometallic Pt and oxidized and reduced monometallic Pd catalysts. The samples were precalcined at 550 °C for 16 h and assessed in the first ignition temperature-programmed reaction. A higher Pt proportion resulted in a lower catalyst activity per gram of metal(s) and surface proportion, as determined by CO chemisorption. The activity drop was too dramatic and could not be explained by the dispersion decrease or structure sensitivity of the reaction. In situ XANES and EXAFS spectroscopy measurements were conducted for Pd, Pt, and Pd–Pt 2:1 catalysts. Monometallic palladium was fully oxidized in the investigated temperature range, whereas the addition of platinum promoted palladium reduction, even under the reactive oxidizing environment. The Pd/PdO weight ratio in bimetallic Pd–Pt 2:1 catalysts decreased from 98/2 to 10/90 in the 200–500 °C temperature range under the reaction conditions. Thus, platinum promoted the formation of a reduced palladium phase, which was significantly less active in the methane combustion reaction than that of oxidized palladium. The study shed light on the effect of platinum on the state of an active palladium surface under low-temperature dry lean methane combustion conditions, which was of importance for methane-emission control devices. Care should be exercised not to extrapolate these findings on the negative effect of platinum on palladium catalyst performance in methane-rich combustion, at different temperature ranges, in the presence of water in the feed (as in automotive converters) and long-term catalyst stability.

Experimental Section

Materials

H_2PtCl_6 (8% w/v solution, Sigma–Aldrich), $Pd(AcO)_2$ (Sigma–Aldrich), 1,4-dioxane (>99.9% Sigma–Aldrich), poly *N*-vinylpyrrolidone (PVP; average molecular weight of 40000, Sigma–Aldrich), ethylene glycol (>99.9%, Fischer Scientific), γ-Al_2O_3 (average pore size 58 Å, specific surface area 155 $m^2 g^{-1}$, 100 μm particle diameter, Sigma–Aldrich), and PdO (99.97% trace metal basis, Sigma–Aldrich) for the in situ EXAFS analysis were used as received. Milli-Q water (18.2 MΩ cm^{-1}) was used.

Catalyst Preparation

Pd and Pt monometallic nanoparticles were synthesized by the one-step alcohol reduction method on the basis of 0.2 mmol metal. To synthesize Pt nanoparticles, H_2PtCl_6 and PVP with a molar ratio of 40 PVP to metal were added to a 500 mL flask and mixed with 80 vol% ethylene glycol in water. In the case of Pd nanoparticle synthesis, $Pd(AcO)_2$ was first dissolved in dioxane (10 mL) and then mixed with the aforementioned amount of PVP and solvent solution. The resulting mixture was stirred and heated until it boiled and then heated at reflux in air under vigorous stirring for 3 h to complete the synthesis of PVP-protected nanoparticles. Bimetallic Pd–Pt nanoparticles were synthesized through the co-reduction of metal precursors with the required molar ratios of Pd/Pt. The rest of the process was exactly the same as that described for the monometallic nanoparticles. A dark colloidal suspension was obtained at the end of synthesis without any precipitates. Nanoparticles were supported on γ-Al_2O_3 by acetone precipitation to obtain 0.3 wt% metal loading. All samples were dried and calcined in air at 550 °C for 16 h. Hereafter, the catalyst after calcination that is ready for the reaction is referred to as the calcined (or oxidized) catalyst.

Catalyst Characterizations

The metal loading on catalysts was determined by NAA. Samples were irradiated for 110 s in the Cd-shielded, epithermal site of the reactor core. They were counted for 30 min each on an Aptec CS11-A31C gamma detector approximately 12 h after irradiation. TEM images were taken with a JEOL-2100 TEM device operating at 200 kV. CO pulse chemisorption analysis was performed with an AutoChem 2920 instrument (Micromeritics, USA). Prior to this analysis, the samples (≈100 mg) were reduced in 25 mL min^{-1} of 10% H_2 in Ar from room temperature to 550 °C at a rate of 20 °C min^{-1}. Then, pulse chemisorption was performed by dosing 3% CO in He at room temperature. The volumetric flow rates of CO in He loop gas and He carrier gas were adjusted to 25 mL min^{-1}. CO uptake per gram of pure support (γ-Al_2O_3) was also evaluated by using 2 g of alumina, which was subtracted from the values for the supported catalysts.

In situ XAS measurements were conducted at Canadian Light Source. Full in situ methane oxidation XAS measurements were

performed for the Pd K edge and Pt L_3 edge on the Hard X-ray MicroAnalysis (HXMA) beamline. The energy range used for the Pd K edge was from 24050 to 25400 eV. Pd K-edge experiments were conducted by using a Si (220) monochromator crystal, Pt mirrors and ion chambers filled with an N_2/Ar gas mixture, whereas Pt L_3-edge spectra were collected by using a Si (111) crystal and Rh mirrors. The samples were loaded into a six-shooter sample cell (Figure 8) as pressed pellets of alumina supports containing about 2 wt% metal elements, and data was collected in transmission mode. The entire setup for the in situ XAS measurements is depicted in Figure 9.

Figure 8. Six-shooter sample holder for in situ XAS data collection. The total diameter of the six shooter is 18 mm, and the diameter of each hole for the sample is 4 mm. The small hole at the top connects to the thermocouple, and the larger central hole is used for beam alignment.

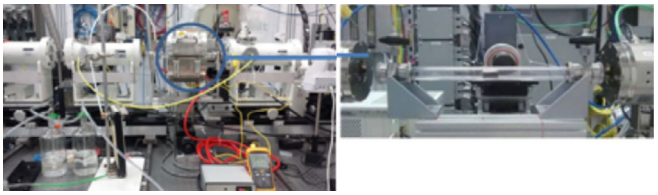

Figure 9. In situ methane oxidation setup at the HXMA beam line (left) and the sample holder in the quartz tube (right). The blue circled part is a small furnace for the in situ XAS measurements, and the sample holder within the quartz tube resides in the furnace.

Initially, calcined mono- and bimetallic samples (Pd and Pd–Pt 2:1) were measured, and then, in situ methane oxidation measurements were conducted. For reference compounds, Pd and Pt foils and PdO were analyzed. Two-dimensional mapping of the sample holder was conducted before the measurement to find the exact location of each sample. The range of mapping was $\pm$15 mm from the zero point by using the motorized setup at the beam line. For methane oxidation under dry conditions, 0.1% CH_4 in N_2 and compressed air (ultrazero level, $<$2 ppm H_2O) were combined. The samples were incrementally heated from 200 to 500 °C under a flow of methane and air in dry conditions. The flow rates of CH_4/N_2 and compressed air used were 154 and 103 mL min^{-1}, respectively.

Linear combination fitting of normalized XANES μ(E) spectra was performed by using the IFEFFIT software package.[43] The XANES spectra of PdO and the reduced Pd sample were used as reference materials, representing the Pd^{II} and Pd^0 species, respectively. Fits were performed on data at each temperature over the range of $-$25 to 65 eV around the absorption edges.

Catalytic Performance in the Methane Combustion Reaction

The methane combustion reaction was studied in a conventional tubular reactor over the monometallic Pd and Pt and bimetallic Pd–Pt nanocatalysts. The reduction of monometallic Pd catalysts was conducted at 350 °C for 2 h under a hydrogen gas stream. Details of the reaction setup were reported previously.[15,44] The reactor with a 0.925 cm internal diameter was packed with catalysts corresponding to 1.2 mg of active Pd. In the case of the monometallic Pt catalyst, 1.2 mg of Pt were used. Then, a gas mixture of 10 vol% CH_4 in nitrogen along with dry air was fed to the reactor at flow rates of 8.5 and 205 mL min^{-1}, respectively, for a CH_4 concentration of about 4000 ppm in the reactor. The composition of the product gas was analyzed by using an online Agilent 7890A gas chromatograph equipped with a thermal conductivity detector (TCD) and a flame-ionization detector (FID). In an ignition test, the temperature was increased stepwise from 200 to 500 °C at the rate of 3 °C min^{-1} and kept at each temperature for 30 min to investigate the catalytic performance in a heating ramp.

The methane conversion and kinetic parameters at 350 °C, as reported in Table 1 and Figure 3, were confirmed to represent intrinsic reaction conditions under isothermal reactor operation. In the most susceptible case of transport limitations for the most active Pd catalyst, Mears criterion for external mass transfer limitations (MTL) was found to be 10^{-4} (no external MTL existed if the value was below 0.15).[45] The Weisz–Prater criterion for internal MTL was found to be 0.32 with Knudsen diffusion-limited pore diffusion, which corresponded to an internal effectiveness factor of 0.97 for a first-order reaction, and thus, negligible internal MTL.[46] The absence of an external temperature gradient was confirmed by Mears correlation (value of 10^{-8}, which was below the maximum limit of 0.15 for the negligible gradient).[45] The maximum internal temperature rise was calculated, by using parameter β, to be 10^{-4} K, assuming an activation energy of 92 kJ mol^{-1}[47] and constant heat of combustion of $-$890 kJ mol^{-1}.

Acknowledgements

Financial support from NSERC (Strategic grant STPGP 430108-12), CFI (Leaders' Opportunity Fund, grant 24766), is appreciated. The X-ray absorption work was performed at the Canadian Light Source, which is supported by the Canadian Foundation for Innovation, Natural Sciences and Engineering Research Council of Canada, the University of Saskatchewan, the Government of Saskatchewan, Western Economic Diversification Canada, the National Research Council Canada, and the Canadian Institutes of Health Research. We thank Dr. John Duke (University of Alberta) for NAA, and Dr. Ning Chen for assistance with XAS measurements on the HXMA beamline.

Keywords: heterogeneous catalysis · nanoparticles · oxidation · reaction mechanism · X-ray absorption spectroscopy

[1] International Energy Outlook 2016, in *US Energy Information Administration, Report number DOE/EIA-0484(2016)*, http://www.eia.gov/forecasts/ieo/pdf/0484(2016).pdf, **2016**, pp. 1–276.
[2] R. Hayes, *Chem. Eng. Sci.* **2004**, *59*, 4073–4080.
[3] S. Su, J. Agnew, *Fuel* **2006**, *85*, 1201–1210.
[4] M. Cargnello, J. J. D. Jaén, J. C. H. Garrido, K. Bakhmutsky, T. Montini, J. J. C. Gámez, R. J. Gorte, P. Fornasiero, *Science* **2012**, *337*, 713–717.

[5] N. M. Kinnunen, J. T. Hirvi, T. Venäläinen, M. Suvanto, T. A. Pakkanen, *Appl. Catal. A* **2011**, *397*, 54 – 61.
[6] R. J. Farrauto, M. C. Hobson, T. Kennelly, E. M. Waterman, *Appl. Catal. A* **1992**, *81*, 227 – 237.
[7] Y.-H. Chin, M. Garcia-Dieguez, E. Iglesia, *J. Phys. Chem. C* **2016**, *120*, 1446 – 1460.
[8] J.-D. Grunwaldt, M. Maciejewski, A. Baiker, *Phys. Chem. Chem. Phys.* **2003**, *5*, 1481 – 1488.
[9] O. Demoulin, M. Navez, E. M. Gaigneaux, P. Ruiz, A.-S. Mamede, P. Granger, E. Payen, *Phys. Chem. Chem. Phys.* **2003**, *5*, 4394 – 4401.
[10] K. I. Fujimoto, F. H. Ribeiro, M. Avalos-Borja, E. Iglesia, *J. Catal.* **1998**, *179*, 431 – 442.
[11] N. M. Kinnunen, J. T. Hirvi, M. Suvanto, T. A. Pakkanen, *J. Mol. Catal. A* **2012**, *356*, 20 – 28.
[12] A. Ersson, H. Kušar, R. Carroni, T. Griffin, S. Järås, *Catal. Today* **2003**, *83*, 265 – 277.
[13] G. Lapisardi, L. Urfels, P. Gélin, M. Primet, A. Kaddouri, E. Garbowski, S. Toppi, E. Tena, *Catal. Today* **2006**, *117*, 564 – 568.
[14] R. Strobel, J.-D. Grunwaldt, A. Camenzind, S. E. Pratsinis, A. Baiker, *Catal. Lett.* **2005**, *104*, 9 – 16.
[15] R. Abbasi, L. Wu, S. E. Wanke, R. E. Hayes, *Chem. Eng. Res. Des.* **2012**, *90*, 1930 – 1942.
[16] E. Becker, P.-A. Carlsson, H. Grönbeck, M. Skoglundh, *J. Catal.* **2007**, *252*, 11 – 17.
[17] C. F. Cullis, B. M. Willatt, *J. Catal.* **1983**, *83*, 267 – 285.
[18] C. H. Bartholomew in *Studies in Surface Science and Catalysis, Vol. 88* (Eds.: B. Delmon, G. F. Froment), Elsevier, Amsterdam, **1994**, pp. 1 – 18.
[19] C. Micheaud, P. Marécot, M. Guérin, J. Barbier, *Appl. Catal. A* **1998**, *171*, 229 – 239.
[20] K. Persson, A. Ersson, K. Jansson, N. Iverlund, S. Järås, *J. Catal.* **2005**, *231*, 139 – 150.
[21] H. Yamamoto, H. Uchida, *Catal. Today* **1998**, *45*, 147 – 151.
[22] K. Narui, H. Yata, K. Furuta, A. Nishida, Y. Kohtoku, T. Matsuzaki, *Appl. Catal. A* **1999**, *179*, 165 – 173.
[23] Y. Deng, T. G. Nevell, *Catal. Today* **1999**, *47*, 279 – 286.
[24] K. Persson, A. Ersson, S. Colussi, A. Trovarelli, S. G. Järås, *Appl. Catal. B* **2006**, *66*, 175 – 185.
[25] Y. Ozawa, Y. Tochihara, A. Watanabe, M. Nagai, S. Omi, *Appl. Catal. A* **2004**, *259*, 1 – 7.
[26] P. Gélin, M. Primet, *Appl. Catal. B* **2002**, *39*, 1 – 37.
[27] Y.-H. Chin, D. E. Resasco, *Catalysis* **1999**, *14*, 1 – 39.
[28] Z. Li, G. B. Hoflund, *J. Nat. Gas Chem.* **2003**, *12*, 153 – 160.
[29] C. B. Alcock, G. W. Hooper, *Proc. R. Soc. London Ser. A* **1960**, *254*, 551 – 561.
[30] H. Zhang, M. Jin, Y. Xia, *Chem. Soc. Rev.* **2012**, *41*, 8035 – 8049.
[31] R. F. Hicks, H. Qi, M. L. Young, R. G. Lee, *J. Catal.* **1990**, *122*, 280 – 294.
[32] K. Persson, A. Ersson, K. Jansson, J. L. G. Fierro, S. G. Järås, *J. Catal.* **2006**, *243*, 14 – 24.
[33] K. Persson, K. Jansson, S. G. Järås, *J. Catal.* **2007**, *245*, 401 – 414.
[34] A. Maione, F. André, P. Ruiz, *Appl. Catal. B* **2007**, *75*, 59 – 70.
[35] A. Dianat, N. Seriani, M. Bobeth, W. Pompe, L. C. Ciacchi, *J. Phys. Chem. C* **2008**, *112*, 13623 – 13628.
[36] A. Dianat, J. Zimmermann, N. Seriani, M. Bobeth, W. Pompe, L. C. Ciacchi, *Surf. Sci.* **2008**, *602*, 876 – 884.
[37] T. R. Johns, J. R. Gaudet, E. J. Peterson, J. T. Miller, E. A. Stach, C. H. Kim, M. P. Balogh, A. K. Datye, *ChemCatChem* **2013**, *5*, 2636 – 2645.
[38] A. Morlang, U. Neuhausen, K. V. Klementiev, F.-W. Schütze, G. Miehe, H. Fuess, E. S. Lox, *Appl. Catal. B* **2005**, *60*, 191 – 199.
[39] C. Carrillo, T. R. Johns, H. Xiong, A. DeLaRiva, S. R. Challa, R. S. Goeke, K. Artyushkova, W. Li, C. H. Kim, A. K. Datye, *J. Phys. Chem. Lett.* **2014**, *5*, 2089 – 2093.
[40] J. L. DuBois, P. Mukherjee, T. D. P. Stack, B. Hedman, E. I. Solomon, K. O. Hodgson, *J. Am. Chem. Soc.* **2000**, *122*, 5775 – 5787.
[41] T. E. Hoost, K. Otto, *Appl. Catal. A* **1992**, *92*, 39 – 58.
[42] Y.-H. Chin, C. Buda, M. Neurock, E. Iglesia, *J. Am. Chem. Soc.* **2013**, *135*, 15425 – 15442.
[43] B. Ravel, M. Newville, *J. Synchrotron Radiat.* **2005**, *12*, 537 – 541.
[44] J. Shen, R. E. Hayes, X. Wu, N. Semagina, *ACS Catal.* **2015**, *5*, 2916 – 2920.
[45] H. S. Fogler, *Elements of Chemical Reaction Engineering*, 4th ed., Pearson Education, Harlow, **2006**, pp. 841 – 842.
[46] M. A. Vannice, *Kinetics of Catalytic Reactions*, Springer, New York, **2005**, p. 240.
[47] F. H. Ribeiro, M. Chow, R. A. Dalla Betta, *J. Catal.* **1994**, *146*, 537 – 544.

Manuscript received: September 9, 2016
Accepted Article published: October 27, 2016
Final Article published: December 15, 2016